doi:10.1006/geno.2001.6621, available online at http://www.idealibrary.com on IDEAL **Article**

Imprinting and Evolution of Two Kruppel-type Zinc-Finger Genes, *ZIM3* and *ZNF264*, Located in the *PEG3/USP29* Imprinted Domain

Joomyeong Kim,[1,2,*] Anne Bergmann,[1] Edward Wehri,[1] Xiaochen Lu,[1] and Lisa Stubbs[1,2]

[1]*Genomics Division, Biology and Biotechnology Research Program, L-441, Lawrence Livermore National Laboratory, 7000 East Avenue, Livermore, California 94551, USA*
[2]*DOE Joint Genome Institute, 2800 Mitchell Drive, Walnut Creek, California 94598, USA*

[*]*To whom correspondence and reprint requests should be addressed. Fax: (925) 422-2282. E-mail: kim16@llnl.gov.*

We have isolated Kruppel-type (C2H2) zinc-finger genes, *ZIM3* (zinc-finger gene 3 from imprinted domain) and *ZNF264*, located downstream of human and mouse *USP29* genes (encoding ubiquitin-specific processing protease 29). In human, both *ZIM3* and *ZNF264* encode zinc-finger proteins with Kruppel-associated box (KRAB) A and B domains at the amino-terminal regions of the predicted proteins. In contrast, mouse *Zim3* and *Zfp264* seem to have lost protein-coding capability based on the lack of open reading frames (ORFs) in their cDNA sequences. In particular, the 3′ end of the *Zim3* transcript overlaps with the coding region of the adjacent gene *Usp29* in an antisense orientation, indicating the conversion of mouse *Zim3* into an antisense transcript gene for *Usp29*. The expression patterns of *ZIM3* and *ZNF264* have been largely conserved between human and mouse, with testis-specific expression of *ZIM3* and ubiquitous expression of *ZNF264*, but high expression levels in adult testes in both species. Our studies also demonstrate that both mouse genes are imprinted with maternal expression of *Zim3* in adult testes and paternal expression of *Zfp264* in neonatal and adult brain. The reciprocal imprinting of two neighboring mouse genes, *Zim3* and *Zfp264*, is consistent with a pattern observed frequently in other imprinted domains, and suggests that the imprinting of these two genes might be coregulated.

INTRODUCTION

The two parental alleles of some mammalian genes are functionally nonequivalent due to genomic imprinting, in which one of the alleles is epigenetically modified and inactivated based on parental origin. More than 30 imprinted genes have been isolated from human and mouse (http://www.mgu.har.mrc.ac.uk/imprinting/imprin-ref.html#impregs); most of these genes are involved in controlling either fetal development or nurturing behaviors [1]. The "genomic imprinting" phenomenon exists in placental mammals and marsupials but not in monotremes (egg-laying mammals) [2,3]. It is therefore believed that imprinting may have coevolved with the unusual reproductive strategy of these animals [1] to balance the potentially conflicting genetic influences on fetal development that are contributed by the two parents [4,5].

Besides monoallelic expression, there are a number of features common to imprinted genes. Many imprinted genes are associated with CpG islands that are hemi-methylated in a manner specific to the parent of origin [6]. Some imprinted genes (including *Gnas1*, *Igf2*, *Igf2r*, *Ube3a*, and *Znf127*) are transcribed bidirectionally, resulting in both sense- and antisense transcripts [7,8]. A number of imprinted genes, including *H19* and *IPW*, are expressed without any coding capability; the final products of these genes are RNAs rather than proteins [6]. Most imprinted genes are clustered with other imprinted genes in discrete chromosomal regions, with reciprocally imprinted gene pairs often found closely juxtaposed; well-known examples include *Igf2/H19* and *Dlk1/Meg3* [9]. Recent studies of the oppositely imprinted *Igf2/H19* pair have demonstrated that the CpG island located upstream of H19 functions as an enhancer-blocking element (insulator) or boundary element, and that a conserved vertebrate zinc-finger gene, *CTCF*, binds to this boundary element and controls the allele-specific expression of *Igf2* and *H19* [10,11].

Mouse chromosome 7 (Mmu7) contains three different imprinted domains located in the proximal, central, and distal regions of the chromosome [12,13]. The central and distal regions of Mmu7 are homologous to two human chromosome regions, 15q13–q11 and 11p15, respectively, which are

0888-7543/01 $35.00

doi:10.1006/geno.2001.6621, available online at http://www.idealibrary.com on IDEAL

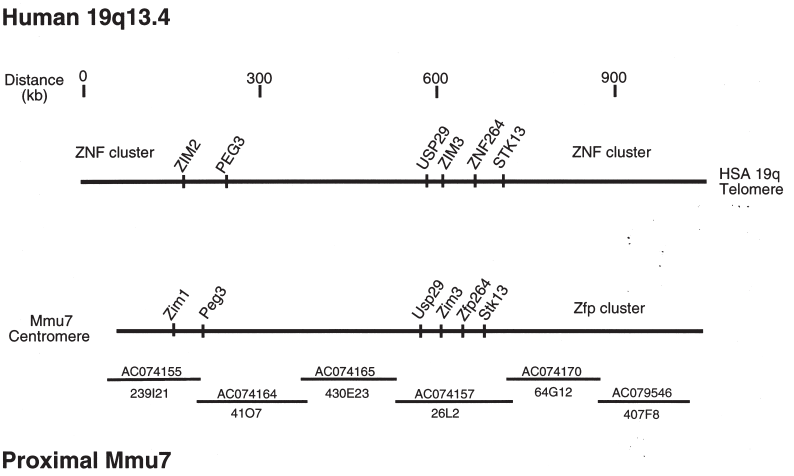

FIG. 1. Comparative map of the human and mouse *PEG3* regions. The upper map represents the 600-kb genomic region of human *PEG3*. The locations of each gene and neighboring zinc-finger gene clusters are indicated. The lower map represents the physical layout of the mouse *Peg3* region. This physical map has been constructed using a large number of overlapping mouse BAC clones (RPCI-23); six sequencing tiling path clones covering this region are indicated by their GenBank accession numbers and clone addresses.

associated with the imprinted genetic disorders Prader-Willi/Angelman [14] and Beckwith-Wiedemann syndromes [15]. The proximal domain contains three previously described imprinted genes: *Peg3* (paternally expressed gene 3) [16], *Zim1* (imprinted zinc-finger gene 1) [17], and *Usp29* [18]. Orthologues of *Peg3* and *Usp29* lie in the homologous region of human chromosome 19q13.4 (HSA19q13.4), but no human gene related to *Zim1* has been found. A second Kruppel-type zinc-finger gene, *ZIM2*, is located downstream of human *PEG3*, and previous studies have shown that human *PEG3* and *ZIM2* share a set of seven, 5′-side exons [19]. As expected, human *PEG3* is also imprinted and is expressed mainly from the paternal allele throughout development and in different tissues [20]. Targeted mutation studies indicate that animals homozygous for *Peg3* null mutations show abnormal parental caring behavior [21], but functions of the more recently discovered proximal Mmu7 imprinted genes are not known.

In a continuing effort to chart the gene content, genomic extent, and evolutionary history of the HSA19q13.4/proximal Mmu7 conserved imprinted domain, we have isolated and characterized two new imprinted zinc-finger genes, *ZIM3* (zinc-finger gene 3 from imprinted domain) and *ZNF264*, both located downstream of *USP29*. The genomic location and structure of *ZIM3* and *ZNF264* are well conserved between human and mouse, and testis-specific expression of *ZIM3* and ubiquitous expression of *ZNF264* are also maintained between the two species. Mouse *Zim3* is transcribed primarily from the maternal allele, whereas mouse *Zfp264* is paternally expressed. Identification of two new imprinted genes, *Zim3* and *Zfp264*, in the region adjacent to *Zim1*, *Peg3*, and *Usp29* confirms the presence of a large imprinted domain in proximal Mmu7/HSA19q13.4.

RESULTS

Isolation of Human and Mouse *ZIM3* and *ZNF264*

As predicted from comparative mapping studies [22], examination of the draft genome sequence of the human 19q13.4 region (NT_000998) identified a number of Kruppel-type zinc-finger (ZNF) genes and a previously described serine threonine kinase gene, *STK13* [23], immediately downstream of *USP29* (Fig. 1). Examination of the genomic sequence between human *USP29* and *STK13* identified two ZNF genes, named *ZIM3* and *ZNF264*. *ZIM3* had no significant nonredundant cDNA or EST matches in

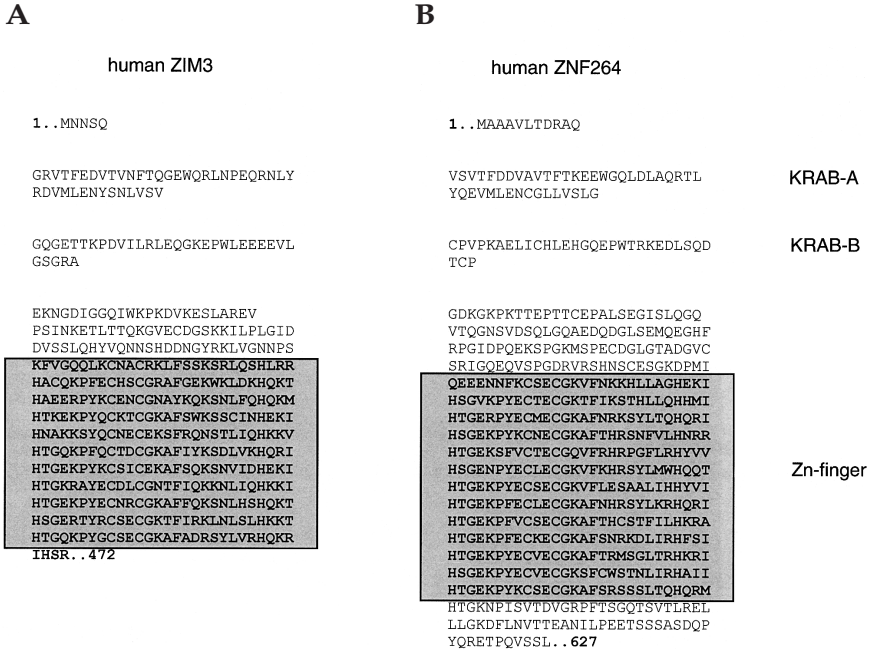

FIG. 2. The amino acid sequence of human *ZIM3* (A) and *ZNF264* (B). KRAB A and B exons are shown and the zinc-finger regions are indicated by shaded boxes.

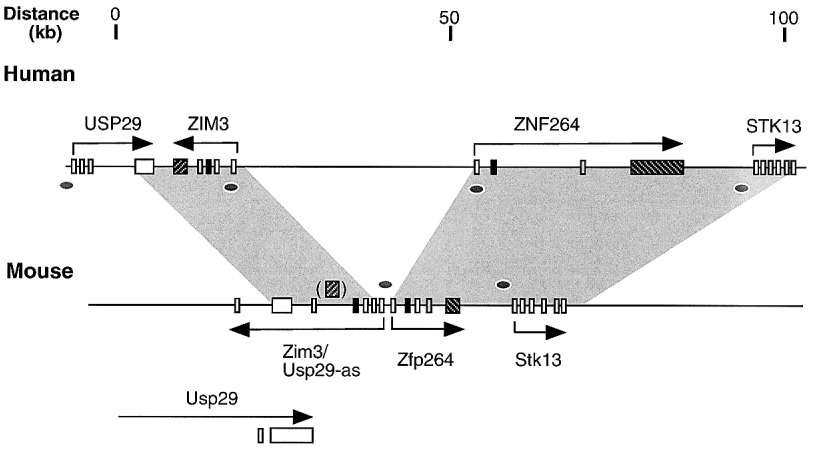

FIG. 3. Genomic organization of human and mouse *ZIM3* and *ZNF264*. The black and gray boxes indicate KRAB A and B exons, respectively. The striped boxes denote zinc-finger exons. The striped box inside a parenthesis indicates the degenerated zinc-finger region of mouse *Zim3*. The CpG islands located in the 5′ side of the genes are indicated by ovals. The transcriptional direction of each gene is indicated by an arrow.

public databases, but *ZNF264* has been cloned as a full-length cDNA (GenBank acc. no. NM_003417). Using RT-PCR and RACE, we cloned a full-length cDNA for human *ZIM3* with a total length of 2.6 kb (GenBank acc. no. AF365931). Analysis of the *ZIM3* cDNA sequence revealed one open reading frame of 472 amino acids and a predicted protein that consists of KRAB A and B motifs linked to a 11-unit zinc-finger domain (Fig. 2A). The 6.5-kb *ZNF264* cDNA encodes a similar 627-amino-acid protein consisting of KRAB A and B motifs and a 13-unit zinc finger domain (Fig. 2B).

A 1-Mb physical map spanning the mouse *Peg3–Usp29* region has been constructed [24] and draft sequence of this region has recently been completed (Fig. 1; P. Dehal, *et al.*, unpublished data). To isolate the mouse homologues of human *ZIM3* and *ZNF264*, we analyzed the draft sequence of one mouse BAC, RPCI-23_26L2 (GenBank acc. no. AC074157), known to contain mouse *Usp29* and *Stk13*. Sequence analysis revealed that this BAC indeed contained two genomic fragments showing high homology with the KRAB A exons of human *ZIM3* and *ZNF264*, respectively. We subcloned and resequenced genomic fragments containing zinc-finger domains from this BAC. The sequence of one genomic fragment, 2 kb in length, was highly homologous to that of human *ZNF264*. With the sequence information derived from these three conserved fragments, we were able to clone cDNA sequences for mouse *Zim3* (3.2 kb in length, GenBank acc. no. AF365932) and *Zfp264* (2.8 kb in length, GenBank acc. no. AF365933).

Careful inspection of *Zim3* and *Zfp264* cDNA sequences yielded two unexpected results. First, although mouse *Zim3* cDNA has a clear KRAB A domain sequence, the cDNA sequence contains no significant ORF and does not encode a clear zinc-finger domain. A degenerated zinc-finger sequence (70% sequence identity with the human *ZIM3*) is located 2 kb downstream of the *Zim3* KRAB A sequence, but KRAB A and finger domains are not included in the same transcript, based on RT-PCR analyses with two flanking oligonucleotide primers (data not shown). On closer inspection, sequences comprising the 3′ end of the *Zim3* cDNA were found to be derived from the coding region of the neighboring gene, *Usp29*, transcribed in an antisense direction (Fig. 3). Second, despite the high level of sequence identity (80% at the nucleotide level) between human and mouse *ZNF264* sequences, the mouse *Zfp264* transcript does not contain a complete ORF due to several stop codons located in the zinc-finger domain of the cDNA sequence. We sequenced *Zfp264* cDNAs derived from several different mouse inbred strains (129/Sv, BALB/c, and C3H) and from a different species (*Mus spretus*), and found the same nonsense mutations in each of those sequences (data not shown). These data confirm that mouse *Zfp264* is no longer capable of encoding a full-length ZNF protein, and that the degeneration of this coding sequence occurred in a common ancestor of *Mus musculus* and *M. spretus*, at least 3 million years ago.

Genomic Structures of Human and Mouse *ZIM3* and *ZNF264*

The genomic structures of human and mouse *ZIM3* and *ZNF264* were analyzed in detail by aligning the sequences derived from cDNAs and the genomic regions (Fig. 3). In human, four genes (*USP29*, *ZIM3*, *ZNF264*, and *STK13*) are localized within a 100-kb genomic region with *ZIM3* transcribed in the opposite direction to that of the other three genes. Human *ZIM3* consists of five exons spanning a 10-kb genomic region, whereas human *ZNF264* consists of four exons covering a 30-kb genomic region. The 5′ ends of both *ZIM3* and *ZNF264* are located adjacent to obvious CpG islands (Fig. 3). The intergenic region between the two genes is estimated to be about 40 kb, and is mainly filled with *Alu* and mammalian-wide interspersed repeat (MIR SINE) elements. The genomic distance between *ZIM3* and *USP29* is estimated to be 6 kb, whereas the distance between *ZNF264* and *STK13* is 10 kb.

Mouse cDNAs representing *Usp29*, *Zim3*, *Zfp264*, and *Stk13* were also compared with the draft sequence (GenBank acc. no. AC074157) of the mouse genomic region. Mouse *Zim3* is composed of seven exons. Exon 4 corresponds to the KRAB A domain, showing 85% sequence identity with the KRAB A domain of human *ZIM3*. Exons 5 and 6, 59 bp and 2.5 kb, respectively, correspond to the antisense exons derived from the coding region of *Usp29*, and exon 7 is derived from an intron of *Usp29*. Independent cDNA screening experiments provided additional confirmation of the relationship between mouse *Usp29* and *Zim3*: two cDNA clones isolated from an

doi:10.1006/geno.2001.6621, available online at http://www.idealibrary.com on IDEAL

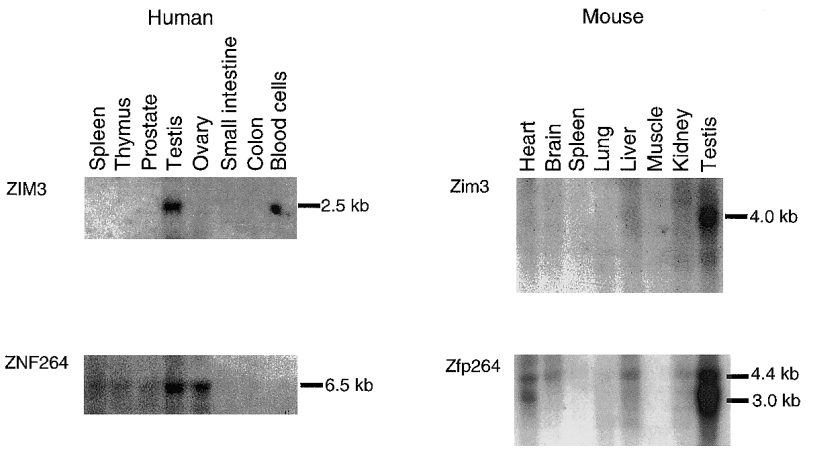

FIG. 4. Northern blot analyses of human and mouse *ZIM3* and *ZNF264*. Human *ZIM3* (top left) and mouse *Zim3* (top right) show testis-specific expression. Both human *ZNF264* (bottom left) and mouse *Zfp264* (bottom right) also show high levels of expression in testes and modest levels in other adult tissues.

adult testis library were very similar in structure to *Zim3* RACE products and represented antisense transcripts of *Usp29*, based on the location of a poly(A) tail in the cDNA sequences. However, the human *ZIM3* cDNA we obtained from this study does not overlap with the transcribed region of human *USP29* (GenBank acc. no. AF229438), and our independent attempts using RT-PCR with primers derived from the transcribed regions of human *USP29* and *ZIM3* yielded no indication that these two genes may overlap in human (data not shown). Mouse *Zfp264* is composed of five exons. Exons 2 and 4 correspond to KRAB A and B domains, showing 83% and 70% sequence identity with those of human *ZNF264*. Exon 3 does not show any similarity with any known sequences, even with human *ZNF264*, and this exon contains in-frame stop codons. Exon 5, encoding the zinc-finger region is estimated to be 2.2 kb, accounting for most of the 2.8-kb cDNA. The 5′ ends of mouse *Zim3* and *Zfp264* are located within 1 kb of each other, and the small genomic region between these two 5′ ends contains a putative CpG island of 300 bp.

Therefore, despite the overall conservation of this genomic interval, several obvious differences distinguish the human and mouse *USP29–STK13* regions. First, the overall sizes of human and mouse genomic intervals are quite different, 100 kb (human) versus 50 kb at maximum (mouse), due mostly to differences in the lengths of the *ZIM3–ZNF264* intergenic regions, which span 40 kb in human and 1 kb in mouse. Second, the individual exons that constitute human and mouse *ZIM3* and *ZNF264* transcripts are quite different. In particular, the two mouse genes seem to have evolved without any evolutionary constraint on protein coding capability. Further, more dramatic changes have also occurred in the rodent lineage; the mouse *Zim3* transcript has become an antisense transcript of *Usp29*, and mouse *Zfp264* has acquired one additional exon with in-frame stop codons as well as several base changes resulting in stop codons in the zinc-finger region.

Expression Patterns of Human and Mouse *ZIM3* and *ZNF264*

To examine the expression patterns of human and mouse *ZIM3* and *ZNF264*, northern blots containing fetal and adult tissue RNAs were hybridized with cDNA probes derived from individual genes (Fig. 4). The human *ZIM3* expression was detected only in adult testes. A cDNA probe derived from the 3′ UTR of human *ZIM3* detected a 2.5-kb transcript, consistent with the size of the *ZIM3* cDNA obtained here. For mouse *Zim3*, a probe corresponding to exons 1 through 3 was used because the 3′ end of the mouse *Zim3* cDNA sequence overlaps with *Usp29*. The *Zim3* probe detected a 4.0-kb transcript with high expression levels in adult testes and low expression levels in 11 and 15 days post coitum (dpc) embryos (data not shown). In contrast to the testis-specific expression of human and mouse *ZIM3*, human and mouse *ZNF264* are both more widely expressed. A cDNA probe derived from the 3′ UTR of human *ZNF264* detected a 6.5-kb transcript in adult testis, ovary, prostate, thymus, and spleen as well as in fetal kidney (data not shown). A cDNA probe of mouse *Zfp264* detected transcripts of 4.4 and 3.0 kb. The highest levels of mouse *Zfp264* expression were detected in adult testes, with relatively low levels of expression detected in heart, brain, liver, and kidney. However, mouse *Zfp264* expression was not easily detectable at the embryonic stage. The expression patterns of *ZIM3* and *ZNF264* are therefore similar but not identical in humans and mice, with testis serving as common sites of primary expression.

In Situ Hybridization of Tissue Sections

The spatial expression patterns of mouse *Zim3* and *Zfp264* were also examined with *in situ* hybridization using sections of 16- and 18-dpc embryos. Besides the relatively testis-specific expression of the two mouse genes in adult tissues, the expression of the two mouse genes was also detected in specific regions of embryos (Fig. 5). The most noticeable expression of both *Zim3* and *Zfp264* occurs in motor neurons and skin. In motor neurons, the expression level of *Zim3* is much higher than that of *Zfp264* (Fig. 5A). In the skin of 16- and 18-dpc embryos, *Zim3* expression was detected in most layers of epidermis and in hair follicles. In contrast, the *Zfp264* expression was detected in only one layer of epidermis, the granular layer (Fig. 5B). Our preliminary data with 14-dpc embryos indicate that the expression of both *Zim3* and *Zfp264* was evident in the interdigital areas of developing limbs, which is somewhat similar to that of *Zim1*, another imprinted zinc-finger gene from this domain (data not shown). Mouse *Zim3* expression was also detected in the hippocampus of 18-dpc embryo brain (data not shown). It is worthwhile to note that

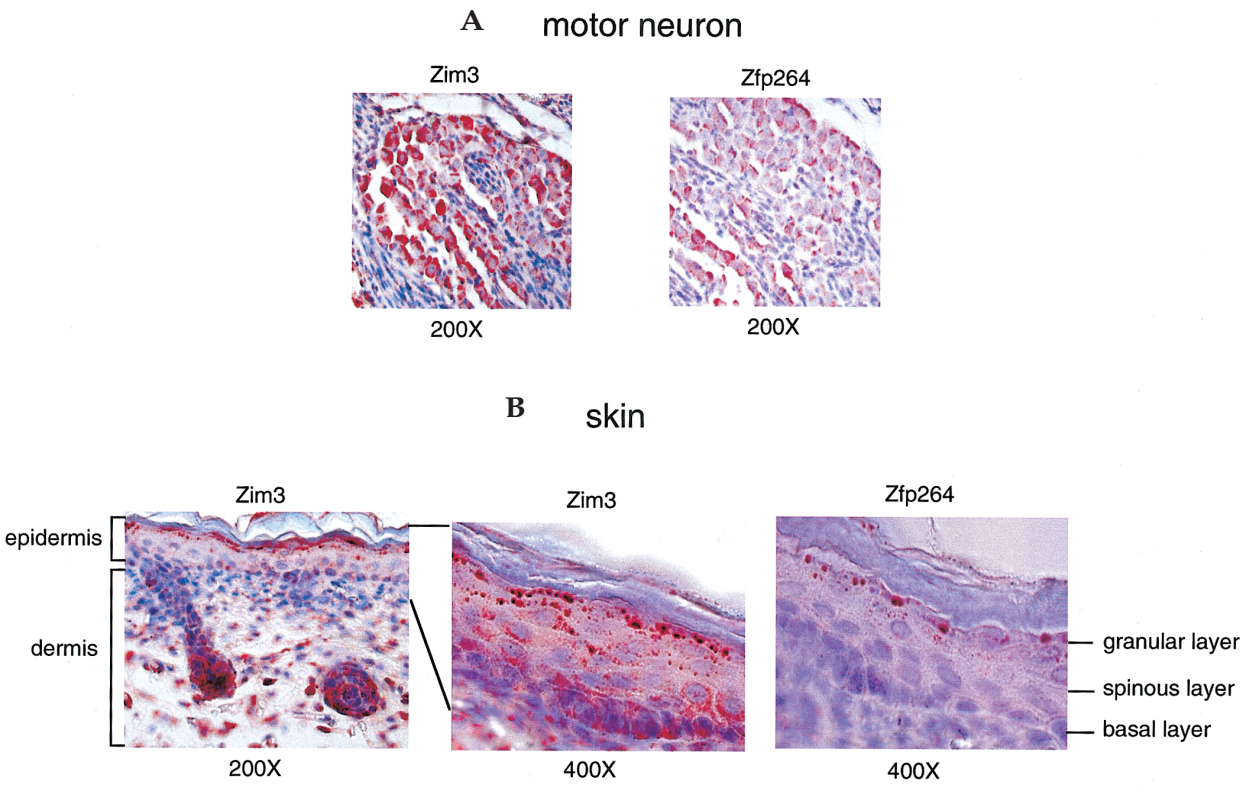

FIG. 5. Section *in situ* hybridization of mouse *Zim3* and *Zfp264*. Sagittal sections of whole 16- and 18-dpc embryos were hybridized with *Zim3* and *Zfp264* probes. Cells expressing the two gene transcripts are stained in red; sectioned tissues have also been counterstained with hematoxylin, which stains nuclei blue. The expression of both *Zim3* and *Zfp264* was detected in motor neurons (A) and skin (B) of 16- and 18-dpc embryos. Relatively high levels of *Zim3* expression were detected in the granular layer of the epidermis and in hair follicles. The hair follicles are circular-shaped regions in the dermis of skin (left panel of B).

the expression levels of both sense and antisense genes, *Usp29* and *Zim3*, are relatively high in embryo brains, but the spatial expression patterns of the two genes are not identical.

Reciprocal Imprinting of *Zim3* and *Zfp264*

To test the imprinting status of mouse *Zim3* and *Zfp264*, we used hybrid animals derived from breeding between *M. musculus* (C3Hf) × *M. spretus* mice [17]. Several sequence polymorphisms that differentiate alleles of each parental species were obtained through comparison of the cDNA sequences derived from *M. musculus* and *M. spretus*. For the imprinting test of mouse *Zim3*, a single base change (nucleotide position 767 in AF365932; C to A in *M. spretus*) in exon 6 was selected because the surrounding 5-base sequence, TCACC, of *M. spretus* is a recognition site for the restriction enzyme *Hph*I, whereas the respective region of *M. musculus*, TCCCC, is not. The amplified cDNA product from testes of F1 adult animals (1 month old) was digested with *Hph*I to measure the ratio of two parental inputs. Expression of mouse *Zim3* is mainly derived from the maternal allele (Fig. 6A). Consistent with restriction enzyme digestion analyses, sequencing of the amplified cDNA product also indicates that most of *Zim3* mRNA is derived from the maternal allele.

The imprinting of *Zfp264* was tested with an insertion/deletion polymorphism located in exon 3, in which the size of the *M. spretus* allele is 70-bp greater than that of the *M. musculus* allele. RT-PCR experiments with RNA derived from testes of 1-week-old and 1-month-old hybrid animals indicated biallelic expression, with slightly more input from the paternal allele in 1-week-old mice (Fig. 6B, lane 6). In contrast, the expression of mouse *Zfp264* in brain is mainly derived from the paternal allele (Fig. 6B, lanes 3 and 4). To confirm this result, a reciprocal analysis was conducted with interspecific backcross progeny (the offspring of an interspecific hybrid female and a C3Hf male; Fig. 6B, lane 5). The result of this test also confirmed the paternal expression of *Zfp264* in brain. Additionally, the imprinting status of mouse *Stk13* was examined, using a sequence polymorphism located in exon 3 of this gene (nucleotide position 645–648 in AF054620; CCGG to CCCG in *M. spretus*). Because of the testis-specific expression of *Stk13* [23], imprinting tests were carried out only with RNA derived from testes. Restriction analysis of amplified cDNA products from different-stage testis RNAs indicates the biallelic expression of mouse *Stk13* in neonatal and adult testes (Fig. 6C, lanes 3–5).

doi:10.1006/geno.2001.6621, available online at http://www.idealibrary.com on IDEAL

DISCUSSION

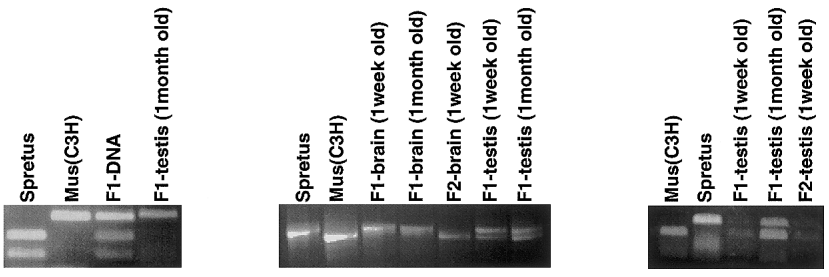

FIG. 6. Imprinting tests of *Zim3*, *Zfp264*, and *Stk13*. (A) Maternal expression of mouse *Zim3* in adult testes (lane 4). (B) Paternal expression of mouse *Zfp264* in the brains of neonates (lanes 3 and 5) and adults (lane 4). (C) Biallelic expression of mouse *Stk13* in the testes of neonates (lanes 3 and 5) and adults (lane 4).

Our data describe the sequence, expression, and evolution of two new zinc-finger genes, *ZIM3* and *ZNF264*, located in chromosome 19q13.4 between *USP29* and *STK13*. Both ZNF genes encode zinc-finger proteins with KRAB A and B domains at the N-terminal regions of the predicted proteins. The mouse homologues of human *ZIM3* and *ZNF264* were isolated from the homologous genomic interval through comparative alignment of the genomic sequences of the two species. Despite the overall conservation of this genomic interval, mouse *Zim3* and *Zfp264* seem to have lost protein-coding capability based on the lack of ORFs in their cDNA sequences. In particular, mouse *Zim3* has become an antisense transcript for *Usp29*, a neighboring imprinted gene. Northern blot analyses indicate that the expression patterns of the two genes have also been conserved between the two species, with testis-specific expression of *ZIM3* and ubiquitous expression of *ZNF264*. The two mouse genes are also shown to be expressed in very specific regions of embryos, such as motor neurons and skins, as illustrated by *in situ* hybridization of late-stage embryo sections. Our studies indicate that both mouse *Zim3* and *Zfp264* are imprinted and expressed primarily from maternal and paternal alleles, respectively. The reciprocal imprinting of these two neighboring mouse genes is reminiscent of a pattern observed in other imprinted domains, and supports the notion that coregulation of such gene pairs is a common feature shared by many imprinted domains.

The discovery of two new imprinted genes, *Zim3* and *Zfp264*, in the region immediately adjacent to *Zim1*, *Peg3*, and *Usp29* is consistent with the observation that, so far, all characterized imprinted genes are clustered in domains. The extent of this imprinted domain in mouse is currently unknown, but the biallelic expression of *Stk13* suggests that the distal boundary in mouse might lie between *Zfp264* and *Stk13* (Fig. 1). Within this imprinted domain, two mouse genes, *Zim1* and *Zim3*, are maternally expressed and three remaining genes, *Peg3*, *Usp29*, and *Zfp264*, are paternally expressed. The 5′ ends of mouse *Peg3* and *Usp29* are located less than 150 bp apart, and similarly the 5′ ends of mouse *Zim3* and *Zfp264* are located within a 1-kb genomic distance. Both mouse *Peg3* and *Usp29* are highly expressed in brain, whereas the two closely located genes *Zim3* and *Zfp264* show highest expression levels in adult testis (Fig. 4). It is possible that the similar expression patterns observed for the pairs *Peg3*/*Usp29* and *Zim3*/*Zfp264* are a result of shared transcriptional regulatory elements; notably, the two genomic regions containing potential regulatory elements for *Peg3*/*Usp29* and *Zim3*/*Zfp264* are close to, or contain, CpG islands. One such island, located in the first intron of *Peg3*, is exclusively methylated on the maternal allele [25], consistent with maternal silencing and paternal expression of *Peg3* and *Usp29*. However, the methylation status of the small CpG island located between the 5′ ends of *Zim3* and *Zfp264* is currently unknown. Studies of other imprinted domains suggest that small genomic regions, termed "imprinting centers" [26], could be responsible for the imprinting of an entire domain [27]. The genomic regions that contain the 5′ ends of the *Peg3*/*Usp29* and *Zim3*/*Zfp264* gene pairs are potential candidates as imprinting centers of this domain, based on proximity to CpG islands, and may also contain regulatory elements necessary for tissue-specific transcription.

Despite its overall conservation, the genomic interval containing *ZIM3* and *ZNF264* seems to have evolved in an unusual fashion. The genomic structure and expression patterns of the two genes are well conserved between human and mouse, and yet the homologous transcripts incorporate different exons and/or have lost their protein coding capability. It is possible that mouse *Zim3* and *Zfp264* have evolved from zinc-finger protein genes to new functional roles as RNA genes. In the case of *Zfp264*, the loss of an ORF seems to have occurred in very recent evolutionary time, based on the high level of sequence similarity still evident between human and mouse *ZNF264*. It is, therefore, uncertain whether mouse *Zfp264* is currently in the process of becoming a pseudogene or an RNA gene. However, the progression of *ZIM3* from a protein-coding gene to an RNA gene, especially as an antisense transcript of the neighboring gene, *Usp29*, seems clearer. The low sequence similarity between the zinc-finger domains of human and mouse *ZIM3*, less than 70%, indicates that mutations resulting in loss of the ORF happened at an early stage of rodent evolution, and yet transcription of *Zim3* has remained active. Although the *in vivo* functions of these antisense transcripts are uncertain, the growing number of identified antisense genes, associated with imprinted domains, strongly implies a significant role in the imprinting process and/or maintenance [7,8].

There have been several cases in which overlapping sense and antisense transcripts are oppositely imprinted, such as *Igf2r/Air* and *Kvlqt1/Lit* [28,29]. Consistent with these examples, the expressed parental alleles for *Zim3* and the neighboring and overlapping gene, *Usp29*, are opposite, with *Zim3* displaying maternal expression and *Usp29* transcribed primarily from the paternal allele [18]. In several documented cases, deletions or mutations that block the transcription of antisense genes resulted in the abolition of imprinting of the sense transcripts [30,31]. It remains to be seen whether *Zim3* transcription might have a similar impact on the transcription of *Usp29*. However, the loss of active protein coding capacity of *Znf264* and the conversion of *Zim3* to an antisense RNA gene, with maintenance of transcriptional activity in both cases, are unique among imprinted domains analyzed so far, and present a very unusual case in general for conserved mammalian genes.

The expression of mouse *Zim3* and *Zfp264* in skin, motor neurons, and inter-digital area of developing limbs is very intriguing. In contrast to other imprinted domains, most of the characterized genes in the proximal Mmu7 and HSA19q13.4 imprinted domains encode Kruppel-type zinc-finger genes, which are predicted to function as transcription factors and are clustered in discrete chromosomal regions [32]. According to recent surveys [32, 33], a large fraction of this gene family is lineage-specific, suggesting that the expansion of this gene family may have happened in recent evolutionary time. Skin, motor neurons, and the interdigital area of developing limbs are formed relatively late in development and thus can accommodate species-specific variations more easily than other regions formed during more critical and rudimentary stages of development [34]. Late lineage-specific expansion events, along with the observed colocalization of several ZNFs to skin and neuronal cells, suggest a role for ZNF genes in the formation of species-specific variants. Although the exact function of this type of gene remains to be determined, the similar expression patterns observed for the three zinc-finger genes (*Zim1*, *Zim3*, and *Zfp264*), at specific regions of embryos, are very unusual. More studies need to be done to test the significance of this pattern and to determine the precise expression sites for the human homologues.

Materials and Methods

cDNA isolation and RACE. A 1.2-kb *ZIM3* cDNA was first amplified from a testis cDNA template (human testis Marathon cDNA template; Clontech, Palo Alto, CA) by two rounds of RT-PCR with two sets of oligonucleotide primers: hZIM3-1 (5′-TAAGTCCTCGCTACCTTCAA-3′) and hZIM3-2 (5′-TGAGGAGGCATGCCTGTCAA-3′), and hZIM3-3 (5′- TGCTCTTCCACAGCTATGAC-3′) and hZIM3-4 (5′- GCGGCTGAATCCCGAACAGA-3′). To obtain 5′ and 3′ ends of *ZIM3*, we carried out RACE [35] with a testis cDNA template. The sequences of oligonucleotides used for 5′- and 3′-RACE are as follows: hZIM3-7 (5′-GACAGGCATGCCTCCTCAGGTGAC-3′) and hZIM3-8 (5′-TCTCCAGCATCACATCCCTGTACA-3′) for 5′-RACE; and hZIM3-5 (5′-CATGGGAAGATATGGTTGCCTGGA-3′) and hZIM3-6 (5′- TGTCACCCCAGAATTCCATGTTGA-3′) for 3′-RACE. The cDNAs of two mouse genes, *Zim3* and *Zfp264*, have also been isolated with 5′- and 3′-RACE experiments using a cDNA template derived from adult testis RNA. The sequences of oligonucleotide used for the 3′-RACE experiment of mouse *Zim3* are as follows: mZim3-3, 5′-GGCCAGGCATAGCGGTACTTGCCT-3′; and mZim3-4, 5′-GCCTATGATTTCAGTACTTGTGAAGT-3′. The sequences of oligonucleotides used for mouse *Zfp264* are as follows: mZfp264-7 (5′- GGGGAACGTATTTGAAGTATTGAG-3′) and mZfp264-8 (5′- GGGAAGACCATGCCATCATCCA-3′) for 3′-RACE; and mZfp264-14(5′-GAAGGCTTTGCCACACTGGAGGCACT-3′) and mZfp264-15 (5′-AAAGGGCTTCTCCCCAGTGTGGA-3′) for 5′-RACE. Amplified RACE products were separated and isolated from a 0.8% agarose gel using a gel extraction column (QIAquick gel extraction kit; Qiagen, Valencia, CA). The isolated PCR products were subcloned into the TA cloning vector (TA cloning kit; Invitrogen, Carlsbad, CA).

Sequencing and sequence analysis. Subcloned cDNA fragments were sequenced from both directions using a fluorescence-based cycle-sequencing DNA sequencing kit (Dye terminator sequencing core kit; PE Applied Biosystems, Warrington, UK) and reactions analyzed on an ABI 377 automated sequencer. Sequence alignments and database searches were carried out using the BLAST program (http://www.ncbi.nlm.nih.gov/BLAST/). For the analyses of genomic sequence derived from mouse and human BACs, two programs were mainly used: Repeat masker ([36]; http://ftp.genome.washington.edu/cgi-bin/RepeatMasker) and PIP (Percent Identity Plot) maker ([37]; http://nog.cse.psu.edu/pipmaker/).

Northern blot analysis. The expression of human and mouse *ZIM3* and *ZNF264* was analyzed with northern blots containing fetal and adult tissue poly(A)$^+$ RNAs (Clontech, Palo Alto, CA). These blots were hybridized with each cDNA probe derived from either 5′- or 3′-UTRs of the genes. The position information of these cDNA probes in the deposit sequences are as follows: *ZIM3*, nt 455–995 in AF365931; *ZNF264*, nt 2341–2720 in NM_003417; *Zim3*, nt 106–418 in AF365932; and *Zfp264*, nt 2057–2376 in AF365933. Detailed procedures and conditions for generating probes and for performing hybridizations have been described [38].

In situ hybridization. To generate antisense RNA probes for *in situ* hybridizations, the transcribed regions of mouse *Zim3* (GenBank acc. no. AF365932, nt 3091–3226) and *Zfp264* (GenBank acc. no. AF365933 nt 798–1115) were used for *in vitro* transcription reactions as described [18]. Antisense probes were labeled with a biotin RNA labeling mix (Boehringer Mannheim, Germany). The hybridization experiments were carried out according to a standard protocol [39] with minimum modifications. The probes were detected by a microscope (BX60, Olympus, Japan) after two rounds of signal amplification using a tyramide signal amplification kit (NEN Life Science, Boston, MA) and staining with a chromogen, aminoethyl carbazole (Zymed, San Francisco, CA). Sectioned tissues were also counterstained using hematoxylin (Zymed, San Francisco, CA). For section *in situ* hybridizations, two different stages of embryos, 16 and 18 dpc, were harvested and fixed with 4% paraformaldehyde. Serial sections, in sagittal planes, were cut at 5 μm.

Imprinting test. The imprinting (or monoallelic expression) of mouse genes was tested with hybrid offspring (F1) produced by crossing *M. musculus* (C3Hf) females with *M. spretus* male mice. The reciprocal imprinting test was carried out with the offspring (F2) produced by backcrossing (*M. musculus* × *M. spretus*) hybrid females with C3Hf males. RNA was isolated using a commercially available kit (Rapid total RNA isolation kit; 5prime-3prime, Inc, Boulder, CO). RNA samples were treated with RNase-free DNase I (Stratagene, La Jolla, CA) for 30 min at 37°C, and 50 μg were used for the synthesis of cDNA (using the cDNA synthesis module; Amersham, Uppsala, Sweden). The final volume of each reverse transcription reaction was 40 μl, and 1 μl of this material was taken for each PCR reaction. The sequences of oligonucleotides used for imprinting tests of mouse *Zim3*, *Zfp264*, and *Stk13* are as follows: mZIM3-5 (5′-GGCCTCTGTGAGTGACAGAG-3′) and mZIM3-6 (5′-GCCGCACTAACACTGAGTTG-3′) for *ZIM3*; Zfp264-1 (5′-AGGAGTGGGGACAGCTGGAC-3′) and Zfp264-2 (5′-TGCACTGGTGGATCTCACTG-3′) for *Zfp264*; and Stk13-I (5′-GGCCCTGAAGGTCCTCTTCA-3′) and Stk13-K (5′-GAGGCCCAGCAGGAGATTCT-3′) for *Stk13*. Each PCR amplification was performed using the following program in a MJ Research PTC-250 instrument: 95°C for 30 s; 60°C for 1 min; 72°C for 1 min for 30 cycles, and 72°C for 5 min for 1 cycle. PCR reactions were carried out in a 50 μl reaction mixture containing 300 ng of each primer, 10 mM Tris-HCl (pH 8.3), 50 mM KCl, 1.5 mM $MgCl_2$, 1 mM dNTPs, 1% Triton X-100, and 1.25 U *Taq* DNA polymerase. Each PCR reaction mixture (10 μl) was separated on 1.8% agarose gels to visualize the amplified PCR products.

For imprinting tests of mouse *Zim3* and *Stk13*, 10 μl of each PCR reaction mixture was digested with 10 units of *Hph*I and *Msp*I, respectively, in a 30 μl reaction, and the digests were examined after separation on 1.8% agarose gels.

ACKNOWLEDGMENTS

We thank Elbert Branscomb (DOE Joint Genome Institute) and Mark Shannon (Molecular Dynamics) for discussions and critical reading of the manuscript, and Todd Coble for technical assistance during in situ hybridization experiments. This work was performed under the auspices of the U.S. Department of Energy by LLNL under contract no. W-7405-ENG-48.

RECEIVED FOR PUBLICATION MAY 25; ACCEPTED JUNE 29, 2001.

REFERENCES

1. Tilghman, S. M. (1999). The sins of the fathers and mothers: genomic imprinting in mammalian development. *Cell* **96:** 185–193.
2. Killian, J. K., *et al*. (2000). *M6P/IGF2R* imprinting evolution in mammals. *Mol. Cell* **5:** 707–716.
3. John, R. M., and Surani, A. M. (2000). Genomic imprinting, mammalian evolution, and the mystery of egg-laying mammals. *Cell* **101:** 585–588.
4. Moore, T., and Haig, D. (1991). Genomic imprinting in mammalian development: a parental tug-of-war. *Trends Genet*. **7:** 45–49.
5. Haig, D. (1993). Genetic conflicts in human pregnancy. *Q. Rev. Biol.* **68:** 495–532.
6. Bartolomei, M. S., and Tilghman, S. M. (1997). Genomic imprinting in mammals. *Annu. Rev. Genet*. **31:** 493–525.
7. Barlow, D. P. (1997). Competition—a common motif for the imprinting mechanism? *EMBO J*. **16:** 6899–6905.
8. Sleutels, F., Barlow, D. P., and Lyle, R. (2000). The uniqueness of the imprinting mechanism. *Curr. Opin. Genet. Dev*. **10:** 229–233.
9. Schmidt, J. V., Matteson, P. G., Jones, B. K., Guan, X. J., and Tilghman, S. M. (2000). The *Dlk1* and *Gtl2* genes are linked and reciprocally imprinted. *Genes Dev*. **14:** 1997–2002.
10. Bell, A. C., and Felsenfeld, G. (2000). Methylation of a *CTCF*-dependent boundary controls imprinted expression of the *Igf2* gene. *Nature* **405:** 482–485.
11. Hark, A. T., *et al*. (2000). CTCF mediates methylation-sensitive enhancer-blocking activity at the *H19/Igf2* locus. *Nature* **405:** 486–489.
12. Searle, A. G., and Beechey, C. V. (1990). Genome imprinting phenomena on mouse chromosome 7. *Genet. Res*. **56:** 237–244.
13. Beechey, C. V., and Cattanach, B. M. (1996). Genetic imprinting map. *Mouse Genet*. **94:** 96–99.
14. Nicholls, R. D., Saitoh, S., and Horsthemke, B. (1998). Imprinting in Prader-Willi and Angelman syndromes. *Trends Genet*. **14:** 194–200.
15. Reik, W., and Maher, E R. (1997). Imprinting in clusters: lessons from Beckwith-Wiedemann syndrome. *Trends Genet*. **13:** 330–334.
16. Kuroiwa, Y., *et al.* (1996). *Peg3* imprinted gene on proximal chromosome 7 encodes for a zinc finger protein. *Nat. Genet*. **12:** 186–190.
17. Kim, J., Lu, X., and Stubbs, L. (1999). *Zim1*, a maternally expressed mouse Kruppel-type zinc-finger gene located in proximal chromosome 7. *Hum. Mol. Genet*. **8:** 847–854.
18. Kim, J., *et al*. (2000). Discovery of a novel, paternally expressed ubiquitin-specific processing protease gene through comparative analysis of an imprinted region of mouse chromosome 7 and human chromosome 19q13.4. *Genome Res*. **10:** 1138–1147.
19. Kim, J., Bergmann, A., and Stubbs, L. (2000). Exon sharing of a novel human zinc-finger gene, *ZIM2*, and paternally expressed gene 3 (*PEG3*). *Genomics* **64:**114–118.
20. Murphy, S. K., Wylie, A. A., and Jirtle, R. L. (2001). Imprinting of *Peg3*, the human homologue of a mouse gene involved in nurturing behavior. *Genomics* **71:** 110–117.
21. Li, L., *et al*. (1999). Regulation of maternal behavior and offspring growth by paternally expressed *Peg3*. *Science* **284:** 330–333.
22. Kim, J., Ashworth, L., Branscomb, E., and Stubbs, L. (1997). The human homolog of a mouse-imprinted gene, *Peg3*, maps to a zinc finger gene-rich region of human chromosome 19q13.4. *Genome Res*. **7:** 532–540.
23. Bernard, M., Sanseau, P., Henry, C., Couturier, A., and Prigent, C. (1998). Cloning of *STK13*, a third human protein kinase related to Drosophila aurora and budding yeast *Ipl1* that maps on chromosome 19q13.3-ter. *Genomics* **53:** 406–409.
24. Kim, J., *et al.* (2001). Homology-driven assembly of a sequence-ready mouse BAC contig map spanning regions related to the 46 Mb gene-rich euchromatic segments of human chromosome 19. *Genomics* (in press).
25. Li, L. L., Szeto, I. Y., Cattanach, B. M., Ishino, F., and Surani, M. A. (2000). Organization and parent-of-origin-specific methylation of imprinted *Peg3* gene on mouse proximal chromosome 7. *Genomics* **63:** 333–340.
26. Nicholls, R. D. (1994). New insights reveal complex mechanisms involved in genomic imprinting. *Am. J. Hum. Genet*. **54:** 733–740.
27. Dittrich, B., *et al.* (1996). Imprint switching on human chromosome 15 may involve alternative transcripts of the *SNRPN* gene. *Nat. Genet*. **14:** 163–170.
28. Lyle, R., *et al*. (2000). The imprinted antisense RNA at the *Igf2r* locus overlaps but does not imprint Mas1. *Nat. Genet*. **25:** 19–21.
29. Mitsuya, K., *et al*. (1999). *LIT1*, an imprinted antisense RNA in the human *KvLQT1* locus identified by screening for differentially expressed transcripts using monochromosomal hybrids. *Hum. Mol. Genet*. **8:** 1209–1217.
30. Wutz, A., *et al*. (1997). Imprinted expression of the *Igf2r* gene depends on an intronic CpG island. *Nature* **389:** 745–749.
31. Horike, S., *et al*. (2000). Targeted disruption of the human *LIT1* locus defines a putative imprinting control element playing an essential role in Beckwith-Wiedemann syndrome. *Hum. Mol. Genet*. **9:** 2075–2083.
32. Shannon, M., Kim, J., Ashworth, L., Branscomb, E., and Stubbs, L. (1998). Tandem zinc-finger gene families in mammals: Insights and unanswered questions. *DNA Seq*. **8:** 303–315.
33. Dehal, P., et al. (2001). Comparison of human chromosome 19 and related regions in mouse: conservative and lineage specific evolution. *Science* **293:** 104-111.
34. Gould, S. J. (1977). *Ontogeny and Phylogeny*. Harvard University Press, Cambridge, Massachusetts.
35. Frohman, M. A., Dush, M. K., and Martin, G. R. (1988). Rapid production of full-length cDNAs from rare transcripts: amplification using a single gene-specific oligonucleotide primer. *Proc. Natl. Acad. Sci. USA* **85:** 8998–9002.
36. Smit, A. F. (1996). The origin of interspersed repeats in the human genome. *Curr. Opin. Genet. Dev*. **6:** 743–748
37. Schwartz, S., *et al*. (2000). PipMaker—a web server for aligning two genomic DNA sequences. *Genome Res*. **10:** 577–586.
38. Stubbs, L., *et al*. (1990). The hox-5 and surfeit gene clusters are linked in the proximal portion of mouse chromosome 2. *Genomics* **6:** 645–650.
39. Hogan, B., Beddington, R., Costantini, F., and Lacy, E. (1994). *Manipulating the Mouse Embryo: A Laboratory Manual*. Cold Spring Harbor Laboratory Press, Cold Spring Harbor, New York.